




Network-Targeted Approach and Postoperative Resting-State Functional Magnetic Resonance Imaging Are Associated with Seizure Outcome

Varina L. Boerwinkle, MD ¹, Emilio G. Cediel, MD,² Lucia Mirea, PhD,³ Korwyn Williams, PhD, MD,¹ John F. Kerrigan, MD,¹ Sandi Lam, MD,⁴ Jeffrey S. Raskin, MD,⁴ Virendra R. Desai, MD,⁵ Angus A. Wilfong, MD,¹ P. David Adelson, MD,^{1,2} and Daniel J. Curry, MD⁶

Objective: Postoperative resting-state functional magnetic resonance imaging (MRI) in children with intractable epilepsy has not been quantified in relation to seizure outcome. Therefore, its value as a biomarker for epileptogenic pathology is not well understood.

Methods: In a sample of children with intractable epilepsy who underwent prospective resting-state seizure onset zone (SOZ)-targeted epilepsy surgery, postoperative resting-state functional MRI (rs-fMRI) was performed 6 to 12 months later. Graded normalization of the postoperative resting-state SOZ was compared to seizure outcomes, patient, surgery, and anatomical MRI characteristics.

Results: A total of 64 cases were evaluated. Network-targeted surgery, followed by postoperative rs-fMRI normalization was significantly ($p < 0.001$) correlated with seizure reduction, with a Spearman rank correlation coefficient of 0.83. Of 39 cases with postoperative rs-fMRI SOZ normalization, 38 (97%) became completely seizure free. In contrast, of the 25 cases without complete rs-fMRI SOZ normalization, only 3 (5%) became seizure free. The accuracy of rs-fMRI as a biomarker predicting seizure freedom is 94%, with 96% sensitivity and 93% specificity.

Interpretation: Among seizure localization techniques in pediatric epilepsy, network-targeted surgery, followed by postoperative rs-fMRI normalization, has high correlation with seizure freedom. This study shows that rs-fMRI SOZ can be used as a biomarker of the epileptogenic zone, and postoperative rs-fMRI normalization is a biomarker for SOZ quiescence.

ANN NEUROL 2019;86:344–356

The incidence of epilepsy is 30 to 50 cases per 100,000 in first-world countries, and double in low-income countries.¹ Nearly 25% of epilepsy cases are drug resistant.² Surgery is the only curative option,^{3–5} but good outcomes depend on accurate localization of the seizure

onset zone (SOZ).⁶ Despite technological advancements, the cure rate is 50 to 80%, depending primarily on etiology.⁷ Thus, improved localization is needed.

Our team first quantitatively described resting-state functional magnetic resonance imaging (rs-fMRI)

View this article online at wileyonlinelibrary.com. DOI: 10.1002/ana.25547

Received Apr 15, 2019, and in revised form Jul 8, 2019. Accepted for publication Jul 9, 2019.

Address correspondence to Dr Boerwinkle, Barrow Neurological Institute at Phoenix Children's Hospital, 1919 E. Thomas Road, Ambulatory Building, Floor 3, Phoenix, AZ 85016. E-mail: vboerwinkle@phoenixchildrens.com

From the ¹Division of Pediatric Neurology, Barrow Neurological Institute at Phoenix Children's Hospital, Phoenix, AZ; ²Division of Pediatric Neurosurgery, Barrow Neurological Institute at Phoenix Children's Hospital, Phoenix, AZ; ³Department of Research, Phoenix Children's Hospital, Phoenix, AZ; ⁴Section of Pediatric Neurosurgery, Riley Hospital for Children, Department of Neurological Surgery, Indiana University School of Medicine, Indianapolis, IN; ⁵Department of Neurosurgery, Houston Methodist Hospital, Houston, TX; and ⁶Department of Pediatric Neurosurgery, Texas Children's Hospital, Baylor College of Medicine, Houston, TX

Additional supporting information can be found in the online version of this article.

localizing epileptogenic or SOZs in the broad pediatric intractable epilepsy population, and showed high correlation with seizure outcome.⁸ In this study, we demonstrated that 75% of Engel I seizure outcomes at 2-year follow-up were achieved in those with rs-fMRI SOZ-targeted destruction. In other studies, preoperative rs-fMRI SOZ localization correlated with stereo-electroencephalography and surgical outcomes.^{9–13}

Despite these advancements, little is known about how surgery modifies the altered neuronal network patterns and if those changes relate to seizure outcome or brain function.^{13–16} Resolution of connectivity abnormalities, in conjunction with seizure freedom, may inform safety in discontinuation of antiseizure medication, liberalization of patient activities and plans, whether or not to surgically pursue anomalous or ambiguous behaviors, or potentiation of long-term improvement in developmental and neuropsychiatric disorders.

Resolution of preoperative connectivity abnormalities in seizure-free children are described in case reports only.^{13,14} For adults, limited cohort studies evaluated the differences between pre- and postoperative rs-fMRI in relation to seizure outcome and have mixed results. The first study evaluated mesial temporal sclerosis and showed postoperative connectivity correlated with seizure freedom.¹⁵ In contrast, another study showed no change in connectivity postoperatively. These authors hypothesized that the connectivity abnormalities in adults were “burned in” by the time surgery occurred.¹⁶

Three important factors may have contributed to these mixed results. First, the initial surgical target of these postoperative studies was the anatomical SOZ, rather than a dysfunctional network as defined by rs-fMRI SOZ. Epilepsy is a network disease,¹⁷ and although anatomical abnormalities visible on magnetic resonance imaging (MRI) may be the location of a true SOZ, it may not show the entire network requiring destruction to achieve seizure freedom. If the rs-fMRI SOZ is the true region requiring destruction, then connectivity abnormalities should resolve postoperatively. Second, it cannot be determined by these prior studies if the reported connectivity abnormalities were the rs-fMRI SOZ or resulted from downstream connectivity disruption, remote from the SOZ. It may be relevant to differentiate between the 2 types of connectivity abnormalities in epilepsy. The crucial factor in seizure freedom may be the resolution and disconnection of the rs-fMRI SOZ rather than the downstream effects, which may take longer to resolve. Lastly, age of onset and years of intractable epilepsy may contribute to the capacity for postoperative plasticity.

To address these questions, rs-fMRI SOZ was prospectively incorporated into presurgical planning for epileptic pediatric patients. Surgery type, location, pre- and

postoperative connectivity changes, as well as patient factors with potential influence on resolution of connectivity abnormalities, were compared with seizure outcomes.

Patients and Methods

The local institutional review board granted prior approval for this hybrid prospective-retrospective study. rs-fMRI has been integrated into standard clinical practice at Phoenix Children’s Hospital and Texas Children’s Hospital for epilepsy surgery evaluation and postoperative management; therefore, no additional consent was deemed necessary for the imaging itself. Each patient’s family and care team were made aware of the procedure and results in the workflow of patient care and multidisciplinary case conference discussion.

Study subjects included pediatric surgical epilepsy patients who received rs-fMRI as part of the preoperative evaluation and then underwent rs-fMRI SOZ-targeted surgery and postoperative rs-fMRI within 6 to 12 months. Baseline data were collected on patient demographics, treating neurologist’s examination, developmental history as reported by family, and epileptologist’s reported patient epilepsy characteristics. The baseline and postoperative MRIs were obtained under standard clinical conditions as described in Boerwinkle et al.⁸

MRI Sequence

Images were acquired on a 3T MRI scanner (Ingenuity; Philips Medical Systems, Best, the Netherlands) equipped with a 32-channel head coil. rs-fMRI parameters included repetition time (TR) = 2,000 milliseconds, echo time (TE) = 30 milliseconds, matrix size = 80 × 80, flip angle = 80°, number of slices = 46, slice thickness = 3.4mm with no gap, in-plane resolution = 3 × 3mm, interleaved acquisition, and number of total volumes = 600, two 10 minute runs totalling 20 minutes. For anatomical reference, a T1-weighted turbo field-echo whole-brain sequence was obtained with the following parameters: TR = 9 milliseconds, TE = 4 milliseconds, flip angle = 8°, slice thickness = 0.9mm, and in-plane resolution = 0.9 × 0.9mm.

Preprocessing

Analysis was carried out similar to Boerwinkle et al⁸ and Mongerson et al¹⁸ using the FMRIB Software Library tool MELODIC.¹⁹ Standard preprocessing steps were applied: the first 5 volumes were deleted to remove T1 saturation effects, high-pass filtering at 100 seconds, slice time correction, without spatial smoothing, and motion corrected by MCFLIRT,²⁰ with nonbrain structures removed. Time courses were variance normalized. Individual functional scans were registered to the patient’s high-resolution anatomical scan using linear registration²¹ and optimized

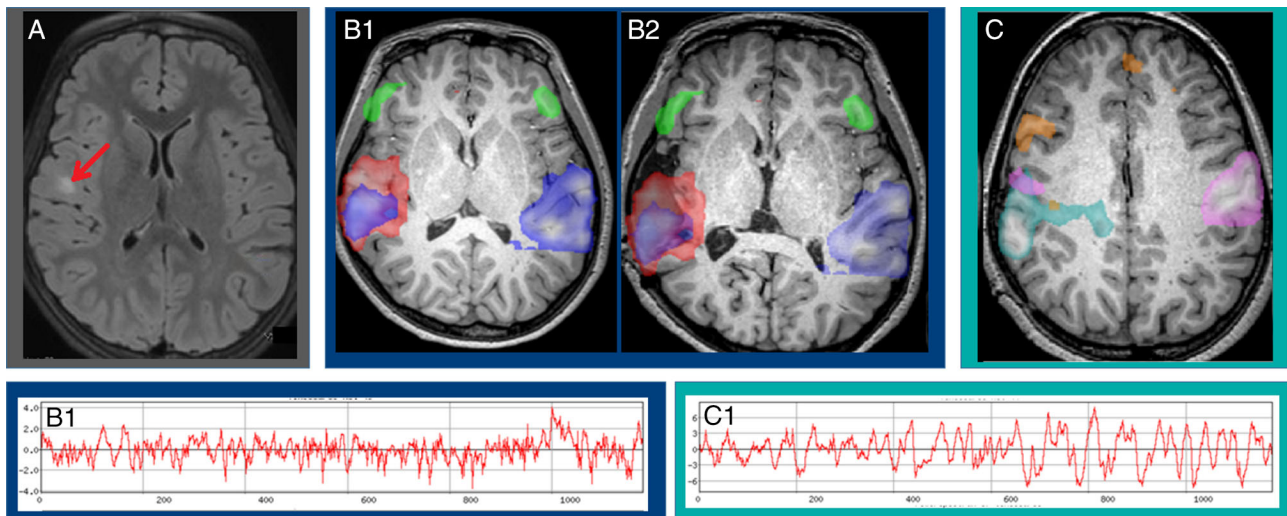


FIGURE 1: This patient had frequent daily seizures preoperatively and was seizure free postoperatively. (A–C) MRI is radiologically oriented. (A) Preoperative T2-weighted image shows focal cortical dysplasia (red arrow). (B1) Preoperative rs-fMRI overlaid on preoperative MRI. Each color is a separate abnormal signal source. The rs-fMRI SOZ is the area of overlap of blue and red areas. The green area is the downstream atypical connectivity. (B2) Same preoperative rs-fMRI, but now coregistered to the postoperative MRI, for viewing in relation to area destroyed. Note that the red-colored signal extends beyond the surgically destroyed area, but the area of overlap, considered the rs-fMRI SOZ, does not. (C) Postoperative rs-fMRI perilesional neuronal signals, shown in teal, pink, and orange, are normalized. Shown below in the red-colored graphs are the corresponding abnormally fast preoperative (B1) and normalized slow postoperative (C1) BOLD time courses. BOLD signal level (y-axis) is plotted against time (x-axis, in seconds). BOLD = blood oxygen level–dependent; MRI = magnetic resonance imaging; rs-fMRI = resting-state functional magnetic resonance imaging; SOZ = seizure onset zone. [Color figure can be viewed at www.annalsofneurology.org]

using boundary-based registration.²² All subjects had <0.5mm head-motion displacement in any direction.

Independent Component Analysis

Overview. Independent component analysis (ICA) is a mathematical process that analyzes the raw rs-fMRI signal and separates it into detected oscillating subsignals. These subsignals, called independent components (ICs), can represent either brain networks or noise. Sources of noise derive from the MRI scanner, respiration, cardiovascular pulsation, and cerebrospinal fluid (CSF) movement. Determining what is noise from the brain networks is described in the literature.^{8,23} Each brain network oscillates in its oxygen concentration independently from the other brain networks, which makes major brain networks distinguishable from each other. Furthermore, the normal time course of this oscillation pattern is smooth and slow (Fig 1). In comparison, abnormal brain networks have faster and more erratic blood oxygen level–dependent (BOLD) time courses (see further detail below).⁸

The preprocessed BOLD sequences underwent multiresolution temporal concatenation. The total number of detected ICs was determined using an established automated dimensionality estimate that utilizes a Bayesian approach.²⁴ As such, the threshold of the ICA was set by the standard local false discovery rate for IC detection at $p < 0.05$.²⁴

rs-fMRI Interpretation

Two blinded reviewers (1 neurologist and 1 neurosurgeon) viewed the ICA results and sorted the ICs into 3 categories—noise, resting-state network, and rs-fMRI SOZ—by the criteria below. If disagreement occurred, discussion between reviewers occurred with an attempt to come to a consensus. If continued disagreement occurred, the plan was to allow a third reviewer (a neurologist) make the final determination.

rs-fMRI interpretation criteria and steps were as follows:

- Noise.** Remove signal due to noise. IC meeting noise criteria: spatially located over major blood vessels, CSF spaces, outside of the brain tissue, or primarily located within white matter; and temporal features consistent with reported norms for noise - primarily $> 0.073\text{Hz}$, and regular oscillation pattern such that the majority of cycles have period changes no greater than half the value of the period between cycles^{8,23,25,26}; or spatial distribution consistent with machine-generated artifact such as skipping slices, or lack of respect for any anatomical boundaries.²³
- Neuronal signal.** Check that all remaining ICs are consistent with neuronal pattern: primarily located within gray matter and are either spatially consistent with established resting-state network (RSN) or undergo further inspection for a rs-fMRI SOZ.

3. **Resting-state networks.** RSNs must be spatially located within the established anatomical regions.^{27,28} The expected detected RSNs are: primary sensory motor networks located in bilateral face area, bilateral leg area, and unilateral right- and left-hand regions; language networks primarily located within left and right inferior frontal gyrus, posterior–superior temporal gyrus, posterior–superior temporal sulcus, posterior–middle temporal gyrus, and supramarginal gyrus; parietal networks primarily located within bilateral homologous parietal gyri, frontal networks primarily located within bilateral premotor, and homologous bilateral frontal gyri; temporal networks primarily located within the bilateral homologous anterior and posterior temporal regions; visual networks located within the bilateral homologous primary and secondary visual association cortices; the default mode network located primarily within the bilateral posterior cingulate gyrus, precuneus, inferior parietal lobules, and medial prefrontal cortex; and the deep gray networks located with the bilateral putamen and bilateral mesial thalami.⁸ Normal RSNs have slow frequency ($<0.073\text{Hz}$ ^{25,26}) and regular oscillation rate (lack interruption from spikes such that change in period is no greater than one-half the period value between cycles).
 4. **Downstream RSN disruption.** If an RSN is spatially overlapping or contiguous with an rs-fMRI SOZ, and oscillation frequency is $>0.073\text{Hz}$, then it meets criteria for RSNs with downstream connectivity disruption. RSNs with downstream disruption may have irregular oscillation features, but will be milder than the frequency disruptions of its overlapping or contiguous rs-fMRI SOZ (50% less change in period between cycles than the rs-fMRI SOZ).
 5. **rs-fMRI SOZ.** Identify preoperative rs-fMRI SOZ⁸ (see criteria below). Incorporate results into surgical planning by multidisciplinary team in conjunction with a clinical battery of preoperative testing including standard electroencephalogram (EEG), intraoperative EEG, positron emission scan, magnetoencephalography, and/or single photon emission computed tomography.
 - a. rs-fMRI SOZ spatial features
 - i. Must be primarily located within gray matter, but not in RSN spatial pattern (see Figs 1–4 for examples).
 - ii. May have a bullseye pattern: 2 or more spatially overlapping abnormal neuronal IC (between 2 and 18 overlapping ICs per patient observed in Texas Children’s Hospital and Phoenix Children’s Hospital data), and may have surrounding and/or overlapping atypical RSN(s). If a bullseye pattern is present, then the area of overlap between the abnormal neuronal IC is considered the most abnormal area and is the rs-fMRI SOZ (see Fig 4).
 - iii. May have alternating-activation deactivation pattern (see Fig 3B3) that is not in typical noise zones (such as arteries, veins, or outside brain), nor detected only in a single slice, or alternating slices or streaks in the phase encoding direction (noise related to MRI sequence, echo-planar imaging susceptibility, or multiband acceleration).²³
 - iv. May have extension toward ventricles through the white matter.
 - v. May have highly irregular borders (see Figs 2–4).
 - b. rs-fMRI SOZ temporal features
 - i. Must contain frequency $>0.073\text{ Hz}$.
 - ii. If a downstream RSN is overlapping or spatially contiguous, then the rs-fMRI SOZ must contain a frequency greater than the RSN.
 - iii. May have irregular oscillation, such as with sharply contoured bursts of irregular runs of faster frequency than baseline with or without gradual return to normal (period change greater than half baseline period between cycles).
6. **Multiple rs-fMRI SOZs.** All rs-fMRI SOZs were reported to the epilepsy team. rs-fMRI SOZs were ranked relative to the individual’s other rs-fMRI SOZs according to the rs-fMRI spatial features. The rs-fMRI SOZ with the highest number of overlapping abnormal neuronal ICs was considered the most abnormal rs-fMRI SOZ. If no overlapping area was detected, then the spatial feature severity rank went according to the order of the remaining list as above (see iii–v). The surgical epilepsy team was also informed of the ranking, and they determined which rs-fMRI SOZ(s), if any, would be targeted for destruction.
7. **Postoperative rs-fMRI SOZ.** Postoperative rs-fMRI underwent analysis of steps 1 to 5.
8. **Postoperative rs-fMRI normalization categorization.** Two blinded reviewers (1 neurologist and 1 neurosurgeon) viewed the postoperative rs-fMRI results, categorizing the rs-fMRI SOZ normalization for each subject. If disagreement occurred, discussion between reviewers occurred with an attempt to come to a consensus. If continued disagreement occurred, the plan was to allow a third reviewer (neurologist) make the final determination.
 - a. No change.
 - i. Preoperative rs-fMRI SOZs remain detected in the postoperative rs-fMRI and are either unchanged in spatial or temporal features *or* do not meet the criteria for improved but indicative of continued epilepsy below.
 - b. Improved but indicative of continued epilepsy.

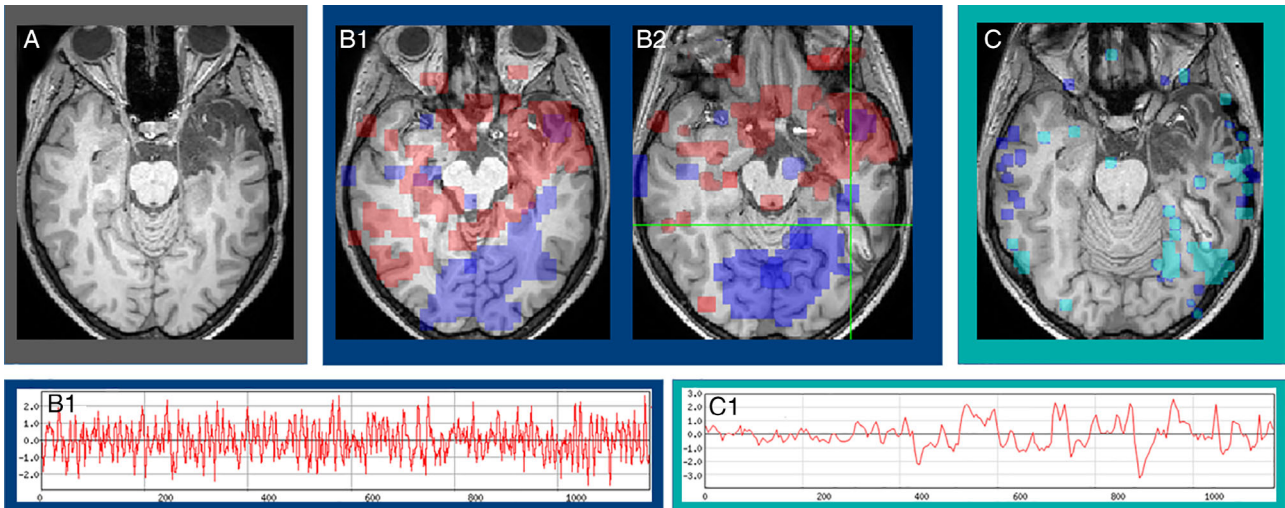


FIGURE 2: This patient had daily visual auras and complex partial seizures despite prior surgery. (A–C) MRI is radiologically oriented. (A) Preoperative T1-weighted image demonstrates prior left anterior lobectomy. (B1) Preoperative rs-fMRI overlaid on preoperative MRI. rs-fMRI SOZ in the remaining left anterior temporal lobe, shown in red, has a downstream separate signal source shown in blue in the vision area, potentially related to the patient’s frequent visual auras. Disconnection surgery by stereotactic laser ablation was performed via 3 trajectories through inferior temporal gyrus, inferior portion of angular gyrus, and lateral parieto-occipital junction. (B2) The same preoperative rs-fMRI, but now coregistered to the postoperative MRI, for visualization next to area destroyed. The green crosshair denotes a representative area of surgical disconnection between the rs-fMRI SOZ (red) and the downstream activity (blue). (C) Postoperative rs-fMRI normalized signal (light blue and dark blue) overlaid on the postoperative MRI. Shown below, B1 and C1 graphs show abnormally fast preoperative and normalized slow postoperative representative BOLD time courses. BOLD signal level (y-axis) is plotted against time (x-axis, in seconds). BOLD = blood oxygen level-dependent; MRI = magnetic resonance imaging; rs-fMRI = resting-state functional magnetic resonance imaging; SOZ = seizure onset zone. [Color figure can be viewed at www.annalsofneurology.org]

- i. Abnormal neuronal signal sources meeting rs-fMRI SOZ criteria, but with >50% reduction in frequency power spectrum above 0.073 Hz and 50% reduction in total number of overlapping signal sources (if found prior) compared to preoperative rs-fMRI SOZs.
- c. Substantial improvement.
 - i. Meets criteria b.i. above.
 - ii. And, no rs-fMRI SOZ with alternating activation–deactivation pattern.
 - iii. And, if RSNs with downstream disruption detected prior, then these remain detected but

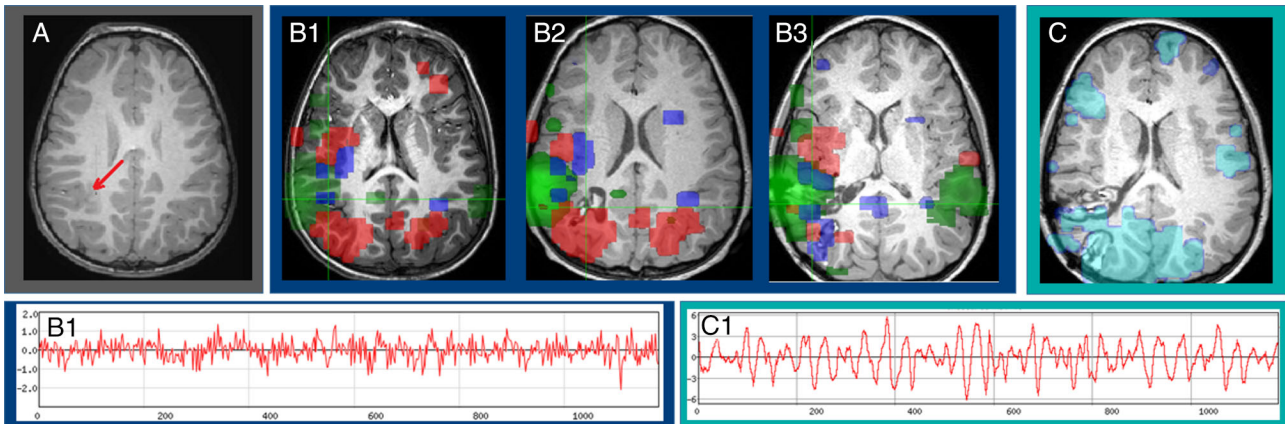


FIGURE 3: This patient had 2 to 5 seizures weekly. (A) Subtle FCD is in right parietal lobe (red arrows). (B1) Preoperative rs-fMRI SOZ is the area of overlap (green crosshair) of the 2 abnormal signal sources (green and the other alternating blue/red) overlaid of preoperative MRI. (B2) Same preoperative rs-fMRI coregistered to postoperative MRI. The initial operation targeted the visible FCD, as shown, but not the rs-fMRI SOZ. There was no reduction in seizures postoperatively for 6 months. (B3) Original preoperative rs-fMRI SOZ (green crosshair) coregistered to MRI done after second surgery. The second surgery did target the rs-fMRI SOZ. Patient then become and remained seizure free at 12 months postoperatively. (C) Normalized final postoperative rs-fMRI (light blue and blue) overlaid on final postoperative MRI. Shown below, B1 and C1 graphs show abnormally fast preoperative and normalized slow final postoperative representative BOLD time courses. BOLD signal level (y-axis) is plotted against time (x-axis, in seconds). BOLD = blood oxygen level-dependent; FCD = focal cortical dysplasia; MRI = magnetic resonance imaging; rs-fMRI = resting-state functional magnetic resonance imaging; SOZ = seizure onset zone. [Color figure can be viewed at www.annalsofneurology.org]

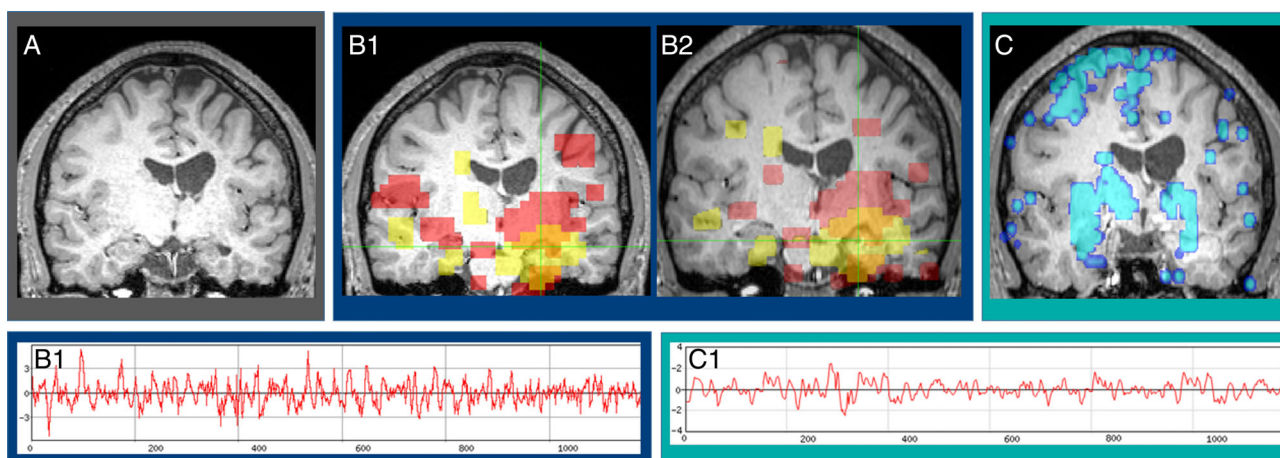


FIGURE 4: This patient had neurodegenerative GSD IV, generalized dystonia, and daily complex partial seizures. (A) Preoperative MRI shows stable left hemispheric atrophy and subtle left hippocampal tail thinning. (B1) Preoperative rs-fMRI SOZ (shown in red and yellow) is the area of overlap of the red and yellow abnormal signal sources, denoted in orange coregistered to preoperative MRI. (B2) Same preoperative rs-fMRI coregistered to postoperative MRI after stereotactic laser ablation of the left hippocampus. (C) Postoperative patient-relative normalized perilesional activity (blue) extends from bilateral putamen to mesial temporal areas, and includes motor cortex. Postoperative normal for this patient is similar to those reported with baseline dystonia and related basal ganglia atypical connectivity. This demonstrates the importance of interpreting the whole-brain rs-fMRI for reliable contextual interpretation, rather than a focused-SOZ-search approach.⁵⁹ Shown below in the red-colored graphs are the corresponding abnormally fast preoperative (B1) and normalized slow postoperative (C1) BOLD time courses. BOLD signal level (y-axis) is plotted against time (x-axis, in seconds). BOLD = blood oxygen level–dependent; GSD = glycogen storage disease type; MRI = magnetic resonance imaging; rs-fMRI = resting-state functional magnetic resonance imaging; SOZ = seizure onset zone. [Color figure can be viewed at www.annalsofneurology.org]

have at least 50% reduction in frequency power spectrum.

- iv. If neither criteria ii nor iii occurred, then categorization remains improved but indicative of continued epilepsy.
- d. Normalized.
 - i. rs-fMRI SOZ no longer detected.
 - ii. And, barring anatomical differences created from surgery, residual detected spatial pattern matching expected RSNs for spatial location.⁸

rs-fMRI Subgroup Analysis. Those patients with a hypothalamic hamartoma received a secondary analysis described in detail in Boerwinkle et al.²⁹ The ICA results were used to filter out noise, and a seed analysis (searchlight analysis [V.L.B.]) within the hamartoma was performed both before and after surgery.²⁹ The preoperative rs-fMRI was registered to the postoperative image anatomical MRI for visual inspection. The postoperative seed was placed over the entire hamartoma and the entire region was reanalyzed, voxel-by-voxel, for connectivity from the HH to the rest of the brain grey matter. The primary author (V.L.B.) interpreted the results, which were checked by 2 neurosurgeons with extensive training in rs-fMRI (J.S.R., V.R.D.). Any difference of opinion was handled with a meeting among investigators. Each patient's full analysis was counted as a single non-overlapping subject.

Surgical Methods

Both institutions' epilepsy-surgery evaluation teams were aligned in their methods of incorporating rs-fMRI into evaluation and treatment. Each standardly acquire preoperative rs-fMRI and incorporated the results along with all other testing and patient demographics. At the team conference, the rs-fMRI results influenced discussion of (1) patient appropriateness as a candidate for surgery, (2) need for and location of intracranial EEG, (3) selection of surgery type (neuromodulation vs destructive; if destructive, then craniectomy vs MRI-guided stereotactic laser ablation; and lesion destructive vs disconnective). Additionally, at both institutions the surgeons were experienced in surgically destroying rs-fMRI SOZs.

It is unknown to what extent rs-fMRI SOZs must be destroyed to stop seizures. When intending to target the rs-fMRI SOZs, the surgeons' approach was to destroy (or disconnect) as much of the rs-fMRI SOZs as possible, taking safety, morbidity, and degree of invasiveness into consideration. Surgical type (as delineated in number 3 above), and surgical intent (ie, to target and destroy as much of the rs-fMRI SOZs as possible vs a palliative approach in which the rs-fMRI is targeted but intentionally left more than 20% intact) were reviewed for analysis.

To determine postoperatively if the rs-fMRI SOZ was destroyed or disconnected, the preoperative rs-fMRI SOZ was coregistered to the postoperative structural image for direct visualization. Two blinded neurosurgeons reviewed

these images retrospectively. The instructions they received were, "It is unknown to what extent SOZ must be destroyed to stop seizures. Was the rs-fMRI SOZ targeted (yes or no)? Was at least 80% of the rs-fMRI destroyed or disconnected?" The ratings were reviewed for consistency, and if disagreement occurred a third rater made the final determination.

Statistical Analyses

Baseline demographics and clinical factors were summarized using count and percent for categorical variables, and the mean and standard deviation or median and interquartile range for quantitative measures. Postoperative rs-fMRI SOZ was classified into 4 categories indicating level of improvement: none, some degree of improvement but abnormalities indicative of continued epilepsy,⁸ substantial, or normalized (as delineated under rs-fMRI Interpretation above).

Similarly, postoperative seizure activity was classified into 4 categories indicating level of seizure reduction: none, $\leq 50\%$ reduction, $>50\%$ reduction but not seizure free, or seizure free. The relationship between categories of postoperative seizure reduction and rs-fMRI improvement was examined using association (Fisher exact test) agreement (weighted κ coefficient) and correlation (Spearman rank correlation coefficient) analyses.

To assess predictive ability, cases that were seizure free and had rs-fMRI normalized were defined as true positives. True negatives were defined as cases with limited seizure reduction (none, $\leq 50\%$, or $>50\%$ but not seizure free) and incomplete rs-fMRI improvement (none, some but still abnormal, substantial). False positive cases included those that were seizure free but rs-fMRI was not normalized, whereas false negative cases included those that were not seizure free but rs-fMRI was normalized. These values were used to estimate sensitivity, specificity, positive predicted value, negative predictive value, and accuracy, as well as corresponding 95% confidence interval.

Further analyses examined the association of patient and clinical factors with seizure reduction and rs-fMRI normalization, using the Fisher exact or Kruskal–Wallis test, as appropriate for the data distribution. To identify factors relating to differences in agreement between postoperative seizure reduction and rs-fMRI improvement, an agreement variable was defined as greater seizure reduction than rs-fMRI improvement, similar extent of seizure reduction and rs-fMRI improvement, and greater rs-fMRI improvement than seizure reduction.

Statistical analyses were performed using the software package SAS version 9.4 (SAS Institute, Cary,

TABLE 1. Patient Characteristics (N = 64)

Age of epilepsy onset and surgery, mo, mean (SD)	22 (33), 117 (63)
Time of onset to surgery, mo, mean (SD)	95 (61)
Male, n (%)	37 (58)
Handedness, left, right, unknown, n (%)	31 (48), 28 (44), 5 (8)
Developmental history, n (%)	
Normal	48 (75)
Developmental delay	15 (23)
Regression	1 (2)
Neurological exam deficit, n (%)	
None	57 (89)
Motor-focal	4 (6)
Combined multiple types	2 (3)
Language impairment alone	1 (2)
MRI classification, n (%)	
Negative	8 (12)
Positive	56 (88)
Primary etiology, n (%)	
Hypothalamic hamartoma	23 (36)
Migrational defect	13 (20)
Familial epilepsy	3 (5)
Tuberous sclerosis	9 (14)
Genetic diagnosis	4 (6)
Mesial temporal sclerosis	3 (5)
Other (etiologies with only 1–2 patients)	13 (20)
Seizure semiology, n (%)	
Generalized tonic clonic	12 (19)
Gelastic	16 (25)
Simple partial	27 (42)
Complex partial	13 (20)
Absence	3 (5)
Atonic	2 (3)
Seizure frequency, weekly average, median (Q1, Q3)	15 (7, 35)
Seizure duration, n (%)	
<5 minutes, ≥ 5 minutes	25 (39), 4 (6)
Broad range, clusters, or indeterminate	35 (55)
No. of antiseizure medications, n (%)	
≥ 1 , but not further specified	44 (69)
2–3, ≥ 4	16 (25), 4 (6)
Surgery type, n (%)	
Focal lesion directed	60 (94)
Nonfocal directed	4 (6)

MRI = magnetic resonance imaging; SD = standard deviation.

TABLE 2. rs-fMRI SOZ Improvement Versus Seizure Reduction

	rs-fMRI SOZ Normalization				Association p^a	Weighted κ Coefficient (95% CI)	Spearman Correlation Coefficient (p)
	None, n = 2	Improved but Still Abnormal, n = 10	Substantial, n = 13	Normalized, n = 39			
Seizure reduction, n (%)					<0.0001	0.71 (0.56–0.86)	0.83 (<0.0001)
No improvement, n = 4	0 (0)	4 (40)	0 (0)	0 (0)			
Reduced \leq 50%, n = 8	0 (0)	5 (50)	3 (23)	0 (0)			
Reduced $>$ 50%, n = 11	0 (0)	1 (10)	9 (69)	1 (3)			
Seizure free, n = 41	2 (100)	0 (0)	1 (8)	38 (97)			
Percent seizure reduction, mean (SD)	100 (0)	22 (28)	72 (28)	99 (4)	<0.0001	—	0.82 (<0.0001)

^a p value from Fisher test or Wilcoxon rank sum test. See Patients and Methods, rs-fMRI SOZ normalization for definition of improvement categories. CI = confidence interval; rs-fMRI = resting-state functional magnetic resonance imaging; SD = standard deviation; SOZ = seizure onset zone.

NC).³⁰ All statistical tests were 2-sided with significance evaluated at the 5% level.

Results

Study subjects included 64 surgical cases among 58 unique individuals (4 patients with 2 surgeries and 1 patient with 3 surgeries). Focus-directed tissue destructive surgery occurred in 60 cases. The remaining 4 cases received either neuromodulation via NeuroPace (Mountain View, CA; 1 patient), vagus nerve stimulation (1 patient), or palliative disconnective surgery via a corpus callosotomy (2 patients).

The mean time from epilepsy onset to surgical intervention was approximately 8 years, despite having, on average, intractable epilepsy from 22 months of age and requiring more than 1 concurrent medication (Table 1). Notably, 8 (12%) cases were nonlesional with a negative anatomical MRI. The ICA approach, as described above, provided robust detection of expected RSNs in all subjects.

Of those with repeat surgery, outcomes were congruent between the rs-fMRI normalization and seizure

improvement, except in 1 case in which rs-fMRI normalized, but seizures were $<$ 50% improved. There was only 1 vagal nerve stimulator case, and the rs-fMRI normalization and seizure outcomes were congruent. No disagreement occurred between rater outcome interpretations.

Review of 60 preoperative rs-fMRI coregistered to postoperative structural imaging confirmed the rs-fMRI SOZ was targeted or disconnected, with 2 exceptions. Two cases did not have rs-fMRI SOZ destruction and correspondingly did not have rs-fMRI normalization, but did have seizure resolution (Table 2) and were considered false positives. The surgeon planned a palliative approach in 9 patients, and these had destruction of the rs-fMRI, but $<$ 80%. In 3 patients, the surgeon intended maximal rs-fMRI SOZ destruction, with $<$ 80% destroyed. The remainder had $>$ 80% rs-fMRI SOZ destruction.

The primary outcome measure, postoperative rs-fMRI SOZ normalization and seizure improvement, demonstrated significant positive correlation (see Table 2). Of 39 cases with postoperative rs-fMRI SOZ normalization,

TABLE 3. rs-fMRI Test in Relation to Seizure Disease

rs-fMRI SOZ	Seizure Present	n	Seizure Absent	n	Total
Positive (not normalized)	True positive	22	False positive	3	25
Negative (normalized)	False negative	1	True negative	38	39
Total		23		41	

rs-fMRI = resting-state functional magnetic resonance imaging; SOZ = seizure onset zone.

38 (97%) became completely seizure free. In contrast, of the 25 cases without complete rs-fMRI SOZ normalization, only 3 (5%) became seizure free. Using binary classification (Table 3), postoperative rs-fMRI SOZ normalization showed high accuracy of 94%, as a test for seizure disease presence, with similarly high sensitivity (96%) and specificity (93%; Table 4).

There were 23 patients with postoperative seizures, of whom 5 (22%) had either corpus callosotomy or neuromodulation. The remaining 18 did have rs-fMRI SOZ at least partially targeted. Twelve of the 18 (67%) these had <80% rs-fMRI SOZ destruction, 9 of which were palliative, and 3 were not. In the remaining 6, 4 had hypothalamic hamartoma with resolution of all seizures except occasional residual gelastic events or auras, 1 was the rs-fMRI SOZ false positive already mentioned (had bilateral MTS with left greater than right abnormal rs-fMRI signals), and the last was an unexplained case of forced normalization alternating with seizures and ongoing rs-fMRI SOZ abnormalities. Thus, of these 23 still seizing, 6 (26%) did have ≥80% rs-fMRI SOZ destruction, but only 2 (9% of those still seizing and 3% of the total study population) had greater than the equivalent of auras or occasional gelastic seizure.

Various configurations of rs-fMRI SOZ target, anatomical lesion, area of operative destruction, and postoperative rs-fMRI were seen. Representative examples of these configurations are displayed in Figures 1–4. For example, some preoperative rs-fMRI SOZs extended beyond a comparatively smaller anatomical lesion (see Fig 1). It was not unusual to see an rs-fMRI SOZ extending far beyond a prior surgical border, prompting the surgical plan to disconnect the remaining major rs-fMRI activation zone (see Fig 2). In an even greater departure from expected, an rs-fMRI SOZ could be found nearby but outside of the

structural lesion (see Fig 3). Highly complex cases (see Fig 4), combining multiple structural pathologies and a metabolic disorder, were encountered and yielded surgical-plan–narrowing information.

The patient characteristics that correlated to rs-fMRI SOZ normalization and seizure improvement were sex and left hemispheric surgery (Supplementary Tables S1a, S1b, and S2). Postoperative rs-fMRI SOZ normalization occurred in significantly more females 21 (54%) relative to males 18 (46%; $p = 0.05$) and higher similarity of seizure and rs-fMRI improvement ($p < 0.05$).

Surgery in the left hemisphere was associated with higher rs-fMRI SOZ normalization ($p = 0.02$, see Supplementary Table S1b), seizure reduction ($p = 0.007$, see Supplementary Table S2), and higher similarity of seizure and rs-fMRI improvement ($p < 0.05$), which was unexpected. More predictably, surgery destroying or focally disconnecting the lesion, rather than neuromodulation or corpus callosotomy, had greater seizure reduction and rs-fMRI SOZ normalization ($p = 0.02$, see Supplementary Table S2).

There was no significant difference between the rate of seizure freedom in those with MRI positive (37 patients; 66% of 56) compared to MRI negative (4 patients; 50% of 8; $p = 0.09$, Supplementary Table S3). Furthermore, the mean age at epilepsy onset or length of time from onset to surgical intervention was not associated with rs-fMRI normalization or seizure improvement ($p = 0.06$, 0.09; see Supplementary Tables S1b and S2b).

Postoperative rs-fMRI improvement was consistent with the extent of seizure reduction for 52 cases (see Supplementary Table S3). rs-fMRI showed greater improvement in 8 patients, whereas seizure reduction was better in the remaining 4 patients.

Discussion

In a pediatric intractable epilepsy population, abnormal rs-fMRI performed well as a biomarker of the epileptogenic zone. Network-targeted surgery, in which the rs-fMRI SOZ destruction was accomplished, is highly associated with seizure resolution and rs-fMRI normalization. Furthermore, a very high surgical seizure freedom rate occurred in the rs-fMRI normalizers (97%).^{31–36} The performance of this biomarker was independent of the presence of visible structural lesion, age of epilepsy onset, and years of epilepsy-time prior to surgery. Sex and hemispheric lateralization may play a role in surgery planning.

Seizure Foci Biomarker and Network-Targeted Approach

The broad population of children with intractable epilepsy have highly variable brain anatomy, localization of seizure

TABLE 4. rs-fMRI Normalization Diagnostic Test Evaluation

	Value	95% CI ^a
Sensitivity	22/23, 95.7%	78.1–99.9%
Specificity	38/41, 92.7%	80.1–98.5%
Positive predictive value	22/25, 88.0%	68.8–97.5%
Negative predictive value	38/39, 97.4%	86.5–99.9%
Accuracy	60/64, 93.8%	84.8–98.3%

^aExact binomial 95% CI.

CI = confidence interval; rs-fMRI = resting-state functional magnetic resonance imaging.

foci, and brain networks. To perform well under these conditions, a biomarker of seizure foci must capture a highly associated physiological marker of epileptogenicity and avoid localization assumptions.

rs-fMRI's capacity to detect SOZ is likely due to the epileptogenic zone's energy drain of brain networks.³⁷ rs-fMRI is a measure of oxygen,³⁸ the carrier of body's energy currency. Seizure energy requirements are far above the basal level.³⁷ The neurons generating seizures send abnormal electrical activity to regions downstream in the network.³⁹ Thus, the epileptic network creates a pattern of abnormal oxygen-dependent connectivity features radiating outward from the epileptogenic bullseye zone. This pattern of energy consumption is likely what allows differentiation of rs-fMRI SOZ from downstream atypical connectivity. rs-fMRI normalization may be an optimal marker of effective rs-fMRI SOZ surgical destruction, and is likely why it resulted in very high seizure resolution. The bullseye epileptogenic center pattern detection is the power of the whole-brain data-driven network-informed surgical approach.

Even when other localization assumptions were avoided, such as assuming the seizure onset zone is localized to abnormalities visible on the anatomical MRI, connectivity assessment performed well as a biomarker of epilepsy resolution. rs-fMRI normalization showed equally good association with seizure freedom in both the structurally MRI-negative and MRI-positive cases. Furthermore, neither the type of lesion nor etiology of epilepsy affected the surgical outcome in this series, in contrast to prior reports.^{7,35} This indicates that rs-fMRI, analyzed by ICA, may be reliable for SOZ detection. This network-targeted approach leads to postoperative rs-fMRI SOZ normalization, which correlates with seizure outcome.

Epilepsy Time

Age of onset and years of epilepsy-time prior to surgery was not associated with rs-fMRI normalization or seizure outcome, despite the finding in other similarly powered surgical studies that demonstrated epilepsy time prior to surgery as associated with poorer outcomes.⁷ The prior authors attributed lack of postoperative rs-fMRI normalization to poor neuroplasticity that is dependent on epilepsy time.¹⁶ However, our findings indicate that this decreased likelihood of rs-fMRI normalization may be due more to lack of a network-targeted approach.

Network-targeted Surgery

Network-targeted-rs-fMRI-SOZ-destroying surgeries, rather than neuromodulation or corpus callosotomy, had greater seizure reduction and rs-fMRI SOZ normalization. Thus, it appears that network-targeted surgery leads to resolution of

abnormal rs-fMRI SOZ-related signals. Yet, to what exact extent rs-fMRI SOZ destruction must occur to lead to seizure cessation remains unclear. In the present study, an arbitrary approximate volume of $\geq 80\%$ of the rs-fMRI SOZs was used as a starting point to begin to define required extent of destruction. The hypothesized bullseye pattern of epileptogenicity within the rs-fMRI SOZ implies that there is a smaller portion of the rs-fMRI SOZ that may be the true epileptogenic zone. Improvement in rs-fMRI acquisition and analysis methods may lead to closer approximations of the true epileptogenic zone. Future studies are needed to more exactly quantify the extent of rs-fMRI SOZ destruction by volumetric analysis, and disconnection by postoperative seed-based analysis of the remaining rs-fMRI SOZ may lead to increased understanding of how rs-fMRI relates to the true epileptogenic zone.

Sex

The trend in demand for precision medicine inspired a deep dive into granular details of patient and surgical characteristics associated with rs-fMRI normalization and better surgical outcome, including gender differences. Previous studies have shown gender differences in neurovascular risk profiles, perfusion scans, and hormonal effects on neuronal and vascular functioning.^{40,41} The gender differences in neurovascular coupling, the basis of the rs-fMRI signal, are prominent enough to differentiate between the different genders.^{42,43} Our data suggest a trend that gender-related rs-fMRI neurovascular coupling differences in surgery and postoperative rs-fMRI in the female brain may lead to better outcomes.

Effect of Laterality

In the present study, left-hemispheric surgeries appeared to have better outcomes in network-targeted surgery. It is likely that there are several confounding variables that may play a role in this apparent association. Examples include gender differences in brain organization,⁴⁴ location-related influences in surgical methodology, differences in surgical treatment, and subhemispheric differences in rs-fMRI network detection attributes,⁴⁵ which may help inform future study design. It remains unclear whether this was a true difference in this study and requires further study to validate this finding.

Strengths

This is the first quantitative study examining pre- and postoperative rs-fMRI as a biomarker of the epileptogenic zone in a large pediatric intractable epilepsy population. It is the first to quantify degree of network-targeting in relation to seizure outcomes. In addition, we demonstrated that postoperative rs-fMRI has a high correlation with seizure outcomes.

A key strength of whole-brain rs-fMRI is that abnormalities are identified within the context of other pathologies creating connectivity disruptions. This is well exemplified in the patient (see Fig 4) with glycogen storage disease and generalized dystonia. After normalization of the rs-fMRI SOZ, the postoperative rs-fMRI demonstrated the expected related effects of dystonia in the basal ganglia and relative depression of connectivity in the left hemisphere. Anticipating whole-brain pathology in this complex population is challenging. Thus, employing a data-driven whole-brain-informed technique allows for a richer context of the brain's connectivity profile, more clinically appropriate interpretation of results, and avoidance of underinformed surgical planning.

Limitations

rs-fMRI ICA derives about 100 images (ICs) with associated time courses per individual, which must then be classified.⁸ Current automated classification schemes perform relatively well in categorizing expected major RSNs.^{46,47} This study's approach appears to be an improvement over current top-down brain-network classifiers trained by data from those with more normal brain function and anatomy, which have yet to demonstrate success in seizure foci localization.^{46,48,49} Thus, similar to all currently employed seizure localization techniques used for presurgical evaluation,⁵⁰ this strategy also relies on interpreter determination of pathogenicity and clinical correlation, and is therefore limited by the same levels and types of subjective bias.^{51,52}

Future Directions

Despite current limitations, seizure focus localization by rs-fMRI holds the promise of further reducing interpreter bias. Advancements have been made in image acquisition and capacity to algorithmically sort images trained by a constellation of image and patient features.^{53–55} It is notable, though, that even the most advanced systems currently rely on “classifier training using expert-hand-labelled data.”⁴⁷ Thus, it is unclear to what extent this could improve upon expert interpretation. However, such algorithms show promise in classifying disease states in individuals.^{56,57}

Difficulties with learning, cognition, depression, or anxiety are well-recognized comorbidities of epilepsy. Connectivity reorganization after seizure cessation may have immediate and long-term improvements.⁵⁸ Tracking the reorganization may reveal which connectivity differences are contributory to ongoing cognition and emotion-control pathology. The impact of this measurable postoperative effect on directing resources and therapies may be high.

A biomarker of brain network normalization linked to seizure freedom is needed to guide postoperative medication management, and should be studied in conjunction with medication wean.

Conclusions

Network-targeted surgery, followed by postoperative rs-fMRI SOZ normalization is highly predictive of seizure freedom, with 94% accuracy, implicating the true biological underpinnings of this test. The independence of this technique's performance from presence of visible MRI lesion, highlights lack of location bias in seizure focus localization. rs-fMRI SOZ normalization may be influenced by sex and hemispheric lateralization, thus may impact risk-benefit surgical stratification.

Author Contributions

All of the authors contributed to conception and design of the study and drafting the text or preparing the figures. V.L.B., E.G.C., L.M., A.A.W., P.D.A., and D.J.C. contributed to acquisition and analysis of data.

Potential Conflicts of Interest

Nothing to report.

References

1. Singh A, Trevick S. The epidemiology of global epilepsy. *Neurol Clin* 2016;34:837–847.
2. Kwan P, Schachter SC, Brodie MJ. Drug-resistant epilepsy. *N Engl J Med* 2011;365:919–926.
3. Engel J, McDermott MP, Wiebe S, et al. Early surgical therapy for drug-resistant temporal lobe epilepsy: a randomized trial. *JAMA* 2012;307:922–930.
4. Fiest KM, Sajobi TT, Wiebe S. Epilepsy surgery and meaningful improvements in quality of life: results from a randomized controlled trial. *Epilepsia* 2014;55:886–892.
5. Wiebe S, Blume WT, Girvin JP, Eliasziw M; Effectiveness and Efficiency of Surgery for Temporal Lobe Epilepsy Study Group. A randomized, controlled trial of surgery for temporal-lobe epilepsy. *N Engl J Med* 2001;345:311–318.
6. West S, Nolan SJ, Cotton J, et al. Surgery for epilepsy. *Cochrane Database Syst Rev* 2015;(7):CD010541.
7. Tonini C, Beghi E, Berg AT, et al. Predictors of epilepsy surgery outcome: a meta-analysis. *Epilepsy Res* 2004;62:75–87.
8. Boerwinkle VL, Mohanty D, Foldes ST, et al. Correlating resting-state functional magnetic resonance imaging connectivity by independent component analysis-based epileptogenic zones with intracranial electroencephalogram localized seizure onset zones and surgical outcomes in prospective pediatric intractable epilepsy study. *Brain Connect* 2017;7:424–442.
9. He X, Doucet G, Pustina D, et al. Presurgical thalamic “hubness” predicts surgical outcome in temporal lobe epilepsy. *Neurology* 2017;88:2285–2293.

10. Qiu T-M, Yan C-G, Tang W-J, et al. Localizing hand motor area using resting-state fMRI: validated with direct cortical stimulation. *Acta Neurochir (Wien)* 2014;156:2295–2302.
11. Zhang CH, Yunfeng L, Brinkmann B, et al. Using functional MRI alone for localization in focal epilepsy. *Conf Proc IEEE Eng Med Biol Soc* 2014;2014:730–733.
12. Zhijuan C, Yang A, Bofeng Z, et al. The value of resting-state functional magnetic resonance imaging for detecting epileptogenic zones in patients with focal epilepsy. *PLoS One* 2017;12:e0172094.
13. Boerwinkle VL, Vedantam A, Lam S, et al. Connectivity changes after laser ablation: resting-state fMRI. *Epilepsy Res* 2018;142:156–160.
14. Li Y, Tan Z, Wang J, et al. Alterations in spontaneous brain activity and functional network reorganization following surgery in children with medically refractory epilepsy: a resting-state functional magnetic resonance imaging study. *Front Neurol* 2017;8:374.
15. Liao W, Ji GJ, Xu Q, et al. Functional connectome before and following temporal lobectomy in mesial temporal lobe epilepsy. *Sci Rep* 2016;6:23153.
16. Maccotta L, Lopez MA, Adeyemo B, et al. Postoperative seizure freedom does not normalize altered connectivity in temporal lobe epilepsy. *Epilepsia* 2017;58:1842–1851.
17. Kramer MA, Cash SS. Epilepsy as a disorder of cortical network organization. *Neuroscientist* 2012;18:360–372.
18. Mongerson CRL, Jennings RW, Borsook D, et al. Resting-state functional connectivity in the infant brain: methods, pitfalls, and potential. *Front Pediatr* 2017;5:159.
19. Beckmann CF, Smith SM. Probabilistic independent component analysis for functional magnetic resonance imaging. *IEEE Trans Med Imaging* 2004;23:137–152.
20. Jenkinson M, Bannister P, Brady M, Smith S. Improved optimization for the robust and accurate linear registration and motion correction of brain images. *Neuroimage* 2002;17:825–841.
21. Jenkinson M, Smith S. A global optimisation method for robust affine registration of brain images. *Med Image Anal* 2001;5:143–156.
22. Greve DN, Fischl B. Accurate and robust brain image alignment using boundary-based registration. *Neuroimage* 2009;48:63–72.
23. Griffanti L, Douaud G, Bijsterbosch J, et al. Hand classification of fMRI ICA noise components. *Neuroimage* 2017;154:188–205.
24. Beckmann CF, DeLuca M, Devlin JT, Smith SM. Investigations into resting-state connectivity using independent component analysis. *Philos Trans R Soc Lond B Biol Sci* 2005;360:1001–1013.
25. Buzsaki G, Draguhn A. Neuronal oscillations in cortical networks. *Science* 2004;304:1926–1929.
26. Zuo XN, Di Martino A, Kelly C, et al. The oscillating brain: complex and reliable. *Neuroimage* 2010;49:1432–1445.
27. Smith SM, Fox PT, Miller KL, et al. Correspondence of the brain's functional architecture during activation and rest. *Proc Natl Acad Sci U S A* 2009;106:13040–13045.
28. Damoiseaux JS, Rombouts SA, Barkhof F, et al. Consistent resting-state networks across healthy subjects. *Proc Natl Acad Sci U S A* 2006;103:13848–13853.
29. Boerwinkle VL, Foldes ST, Torrisi SJ, et al. Subcentimeter epilepsy surgery targets by resting state functional magnetic resonance imaging can improve outcomes in hypothalamic hamartoma. *Epilepsia* 2018;59:2284–2295.
30. SAS Statistical Software [computer program]. Version 9.4. Cary, NC: SAS Institute, 2008.
31. Sharma P, Hussain A, Greenwood R. Precision in pediatric epilepsy. *F1000Res* 2019;8.
32. Plummer C, Vogrin SJ, Woods WP, et al. Interictal and ictal source localization for epilepsy surgery using high-density EEG with MEG: a prospective long-term study. *Brain* 2019;142:932–951.
33. Delev D, Oehl B, Steinhoff BJ, et al. Surgical treatment of extratemporal epilepsy: results and prognostic factors. *Neurosurgery* 2019;84:242–252.
34. Stamoulis C, Connolly J, Axeen E, et al. Noninvasive seizure localization with ictal single-photon emission computed tomography is impacted by preictal/early ictal network dynamics. *IEEE Trans Biomed Eng* 2018. 66: 1863–1871.
35. Choi SA, Kim SY, Kim H, et al. Surgical outcome and predictive factors of epilepsy surgery in pediatric isolated focal cortical dysplasia. *Epilepsy Res* 2018;139:54–59.
36. Steriade C, Martins W, Bulacio J, et al. Localization yield and seizure outcome in patients undergoing bilateral SEEG exploration. *Epilepsia* 2019;60:107–120.
37. Williamson A, Patrylo PR, Pan J, et al. Correlations between granule cell physiology and bioenergetics in human temporal lobe epilepsy. *Brain* 2005;128:1199–1208.
38. Biswal BB, Van Kylene J, Hyde JS. Simultaneous assessment of flow and BOLD signals in resting-state functional connectivity maps. *NMR Biomed* 1997;10:165–170.
39. Boerwinkle VL, Wilfong AA, Curry DJ. Resting-state functional connectivity by independent component analysis-based markers corresponds to areas of initial seizure propagation established by prior modalities from the hypothalamus. *Brain Connect* 2016;6:642–651.
40. Ghisleni C, Bollmann S, Biason-Lauber A, et al. Effects of steroid hormones on sex differences in cerebral perfusion. *PLoS One* 2015;10:e0135827.
41. Roof RL, Hall ED. Gender differences in acute CNS trauma and stroke: neuroprotective effects of estrogen and progesterone. *J Neurotrauma* 2000;17:367–388.
42. Nini M, Hongna Z, Zhiying L, et al. Gender differences in dynamic functional connectivity based on resting-state fMRI. *Conf Proc IEEE Eng Med Biol Soc* 2017;2017:2940–2943.
43. Zhang C, Dougherty CC, Baum SA, et al. Functional connectivity predicts gender: evidence for gender differences in resting brain connectivity. *Hum Brain Mapp* 2018;39:1765–1776.
44. Tian L, Wang J, Yan C, He Y. Hemisphere- and gender-related differences in small-world brain networks: a resting-state functional MRI study. *Neuroimage* 2011;54:191–202.
45. Wang D, Buckner RL, Liu H. Functional specialization in the human brain estimated by intrinsic hemispheric interaction. *J Neurosci* 2014;34:12341–12352.
46. Hacker CD, Laumann TO, Szrama NP, et al. Resting state network estimation in individual subjects. *Neuroimage* 2013;82:616–633.
47. Griffanti L, Salimi-Khorshidi G, Beckmann CF, et al. ICA-based artefact removal and accelerated fMRI acquisition for improved resting state network imaging. *Neuroimage* 2014;95:232–247.
48. Roland JL, Griffin N, Hacker CD, et al. Resting-state functional magnetic resonance imaging for surgical planning in pediatric patients: a preliminary experience. *J Neurosurg Pediatr* 2017;20:583–590.
49. Leuthardt EC, Guzman G, Bandt SK, et al. Integration of resting state functional MRI into clinical practice—a large single institution experience. *PLoS One* 2018;13:e0198349.
50. Itri JN, Patel SH. Heuristics and cognitive error in medical imaging. *AJR Am J Roentgenol* 2018;210:1097–1105.
51. Gunderman RB. Biases in radiologic reasoning. *AJR Am J Roentgenol* 2009;192:561–564.
52. Bruno MA, Walker EA, Abujudeh HH. Understanding and confronting our mistakes: the epidemiology of error in radiology and strategies for error reduction. *Radiographics* 2015;35:1668–1676.
53. Ruiz E, Ramirez J, Gorris JM, Casillas J; Alzheimer's Disease Neuroimaging Initiative. Alzheimer's disease computer-aided diagnosis: histogram-based analysis of regional MRI volumes for feature selection and classification. *J Alzheimers Dis* 2018;65:819–842.

54. Ceschin R, Zahner A, Reynolds W, et al. A computational framework for the detection of subcortical brain dysmaturity in neonatal MRI using 3D convolutional neural networks. *Neuroimage* 2018;178:183–197.
55. Noguchi T, Higa D, Asada T, et al. Artificial intelligence using neural network architecture for radiology (AINNAR): classification of MR imaging sequences. *Jpn J Radiol* 2018;36:691–697.
56. Bouts M, Moller C, Hafkemeijer A, et al. Single subject classification of alzheimer's disease and behavioral variant frontotemporal dementia using anatomical, diffusion tensor, and resting-state functional magnetic resonance imaging. *J Alzheimers Dis* 2018;62:1827–1839.
57. de Vos F, Koini M, Schouten TM, et al. A comprehensive analysis of resting state fMRI measures to classify individual patients with Alzheimer's disease. *Neuroimage* 2018;167:62–72.
58. Tang Y, Xia W, Yu X, et al. Short-term cerebral activity alterations after surgery in patients with unilateral mesial temporal lobe epilepsy associated with hippocampal sclerosis: a longitudinal resting-state fMRI study. *Seizure* 2017;46:43–49.
59. Li Z, Prudente CN, Stilla R, et al. Alterations of resting-state fMRI measurements in individuals with cervical dystonia. *Hum Brain Mapp* 2017;38:4098–4108.